PCCP

Self-association and complex formation in alcohol-unsaturated hydrocarbon systems

Heat capacities of linear alcohols mixed with alkenes and alkynes

Susana Figueroa-Gerstenmaier, Albertina Cabañas† and Miguel Costas*

Laboratorio de Termofisica, Departamento de Fisica y Quimica Teorica, Facultad de Quimica, Universidad Nacional Autonoma de Mexico, Mexico D.F. 04510, Mexico.
E-mail: costasmi@servidor.unam.mx

Received 19th November 1998, Accepted 16th December 1998

Apparent molar heat capacities, C_m^{app}, at dilute alcohol concentrations and excess molar heat capacities, C_p^E throughout the concentration range were determined at 25 °C for the following systems: methanol, ethanol, propan-1-ol, hexan-1-ol and decan-1-ol mixed with *n*-octane, oct-1-ene and oct-1-yne; in addition, the following mixtures were also measured: hexan-1-ol with oct-4-yne, cyclohexane, cyclohexene, benzene, hex-1-ene, dec-1-ene and an equimolar mixture of *n*-octane + oct-1-yne. The experimental C_m^{app} show a maximum against alcohol concentration; this maximum is reduced in magnitude and displaced to higher alcohol concentrations when the inert *n*-octane is substituted by the unsaturated oct-1-ene, oct-1-yne, oct-4-yne, cyclohexene or benzene which act as weak proton acceptors, forming complexes or cross-associated species with the alcohol molecules. The present data clearly indicate that there are alcohol–alkene complexes in solution, which are weaker than the alcohol–alkyne ones, but detectable through heat capacity measurements. The C_m^{app} data for alkan-1-ols when plotted against ψ_1, the concentration of hydroxyl groups in the mixture, follow a single corresponding states curve for each of the solvents. For all alkan-1-ols, C_p^E display the following behaviour: C_p^E (oct-1-yne) < C_p^E (oct-1-ene) < C_p^E (*n*-octane) at low alcohol concentrations and C_p^E (oct-1-yne) > C_p^E (oct-1-ene) > C_p^E (*n*-octane) at higher alcohol concentrations, the cross-over point being between 0.1 and 0.2 alcohol mole fraction. To interpret the data, the Treszcanowicz–Kehiaian (TK) model for associated liquids has been used. The parameters of the model, *i.e.* volumetric equilibrium constants and enthalpies of formation for alcohol–unsaturated hydrocarbon 1 : 1 complexes have been fitted to the dilute alcohol data. With these parameters, the TK model is able to give correct qualitative predictions of the C_p^E results throughout the concentration range. Using the Flory lattice model, the volumetric equilibrium constants were transformed into a unique or intrinsic equilibrium constant, which is independent of molecular size and describes the alcohol–alkene and alcohol–alkyne association. A detailed analysis of the data for hexan-1-ol + oct-1-yne and hexan-1-ol + oct-4-yne indicates that the dominating interaction in the formation of the alcohol–unsaturated hydrocarbon complex is that occurring between the proton of the hydroxy group of the alcohol and the negative electron density in the double or triple bond, producing what can be termed a H-bond. Using the parameters obtained when analyzing excess volumes V^E and excess enthalpies H^E for similar and common systems (T. M. Letcher *et al.*, *Fluid Phase Equilib.*, 1995, **112**, 131), the ERAS model was used to predict C_p^E, finding that it is unable to give a satisfactory rendering of the present heat capacity data.

Self-association of linear alcohols in inert solvents (linear hydrocarbons) has been studied using a wide variety of techniques and several models. When a non-inert or active solvent is employed, other equilibria in solution are established such that alcohol self-association competes with the formation of complexes or cross-associated species between the alcohol and the active solvent molecules. The presence of these cross-associated species modifies substantially the concentration dependence of the thermodynamic properties of the mixture; in particular, it has been found that heat capacity measurements are a good tool to study in detail the processes of self-association and complex formation occurring in the solution.[1–9] Using heat capacities, it has been possible to characterize complexes with enthalpies of formation which are of the same order of magnitude as those of the formation of the alcohol self-associated species, *i.e.*, in the range 18 to 25 kJ mol^{-1}, as for example the complexes formed between alcohol and ester molecules.[6–8] In order to determine if heat capacity measurements can also characterize the formation of weaker complexes, in this work we have studied the alcohol self-association and possible formation of weak alcohol–solvent cross-associated species for a series of linear alcohols mixed with unsaturated hydrocarbons, *viz.* alkenes and alkynes. In order to analyze the data, we have used the Treszczanowicz–Kehiaian (TK) model for associated mixtures. This model has been extensively used[1–9] to interpret heat capacity data for many monoalcohols (linear, branched, cyclic and phenols) and 1,2-diols in inert solvents (alkanes) and in proton-acceptor solvents. The TK model only takes into account the so-called "chemical contributions" to the thermodynamic properties, *i.e.*, those arising from the association or dissociation processes, and hence is unable to predict correctly excess enthalpies or excess volumes. However, it is particularly well suited to analyze heat capacity data where the chemical contributions are dominant and, as it will be seen in detail below,

† Permanent address: Departamento de Quimica-Fisica, Facultad de Ciencias Quimicas, Universidad Complutense, Madrid 28040, Spain.

Table 1 Parameters A_i and standard deviations σ (J K^{-1} mol^{-1}) for representation of the molar excess heat capacities at 25 °C by eqn. (2) or (3)

	A_1	A_2	A_3	A_4	σ
Methanol +					
Oct-1-ene[a]	3.14	0.11513	29.09	0.84281	0.20
Oct-1-yne[b]	48.62	−28.76	30.02		0.52
Ethanol +					
n-Octane[a]	1.68	0.07294	24.46	0.64663	0.06
Oct-1-ene[a]	3.59	0.12639	30.95	0.80825	0.12
Oct-1-yne[b]	60.90	−28.80	27.95		0.46
Propan-1-ol +					
n-Octane[a]	2.09	0.08295	32.08	0.73055	0.03
Oct-1-ene[a]	4.14	0.13856	39.55	0.88119	0.19
Oct-1-yne[b]	69.53	−27.69	26.16		0.74
Hexan-1-ol +					
n-Octane[a]	2.52	0.08923	28.59	0.82506	0.13
Oct-1-ene[a]	4.31	0.13497	35.44		0.04
Oct-1-yne[b]	57.30	−26.24	28.36		0.49
Oct-4-yne[b]	49.62	−20.09	30.42	24.55	0.20
Hex-1-ene[a]	3.12	0.11716	29.68		0.17
Dec-1-ene[a]	6.95	0.16945	41.10	1.24474	0.24
Cyclohexane[a]	1.78	0.08188	16.72	0.77973	0.10
Cyclohexene[a]	4.05	0.14238	25.92		0.17
Benzene[b]	41.84	−15.44	24.16	−20.97	0.41
Decan-1-ol +					
n-Octane[a]	3.08	0.10736	9.18	0.64882	0.07
Oct-1-ene[a]	6.49	0.17710	12.77		0.22
Oct-1-yne[b]	42.62	−28.31	27.47		0.49

[a] Using eqn. (3). [b] Using eqn. (2).

provides valuable insight into the microscopic behaviour of mixtures where association–dissociation equilibria are present.

Similar alcohol–alkene and alcohol–alkyne systems have been studied recently through the measurement of the excess volumes V^E and excess enthalpies H^E.[10–13] Letcher *et al.* applied the extended real associated solution (ERAS) model to the data[14] and found that (i) it is not necessary to consider the association between the alcohol and the alkene molecules, *i.e.*, the alkene behaves as an *n*-alkane or inert solvent and (ii) there is association between the alcohol and the alkyne molecules; this cross-association is proposed to be between the oxygen atom of the alcohol and the acid proton attached to the carbon atom where the triple bond is located. It appeared then interesting to determine, as an additional goal of this work, if the heat capacity measurements reported here corroborate the conclusions reached in ref. 14, and to test the performance of the ERAS model with these data. As will be discussed in detail below, we found that both alkenes and alkynes form complexes with the linear alcohols and that this cross-association mainly occurs between the hydrogen atom of the hydroxy group of the alcohol and the high electron densities of the double and triple bonds in the unsaturated hydrocarbons.

Experimental

Heat capacities at constant pressure at dilute alcohol concentrations (mole fraction less than 0.1) and throughout the concentration range were determined in independent experiments at 25 °C for the following fourteen systems: methanol, ethanol, propan-1-ol, hexan-1-ol and decan-1-ol mixed with *n*-octane (except methanol), oct-1-ene and oct-1-yne. In addition, the following seven mixtures were also measured: hexan-1-ol mixed with oct-4-yne, cyclohexane, cyclohexene, benzene, hex-1-ene, dec-1-ene (only throughout the concentration range) and with a binary equimolar mixture of *n*-octane + oct-1-yne (only dilute alcohol concentrations).

Materials and methods

All chemicals were obtained from Aldrich with purities ranging from 97 to 99.8% (except dec-1-ene with a purity of 94%) and were used without further purification. Volumetric heat capacities were measured using a Picker flow microcalorimeter (Sodev Inc., Sherbrooke, P.Q., Canada) with a precision of 1×10^{-4} J K^{-1} cm^{-3}, and were transformed to a molar basis through solution densities obtained using a vibrating-cell densimeter (Sodev). The instrumentation and procedures have been described in the literature.[15] The temperature was controlled within 0.001 °C using a CT-L thermostat (Sodev). Solutions were prepared by weight (Mettler AT-250 with a 1×10^{-5} g precision) and extreme care was taken during their preparation and handling in order to minimize evaporation losses. In the flow calorimeter, the volumetric heat capacity of the liquid flowing through the working cell is measured against that of the reference cell. For the extremely dilute alcohol concentration, the heat capacity of each solution was determined using the pure solvent as reference. The heat capacity of all pure components were either determined here using *n*-octane as the reference or taken from the literature. At higher alcohol concentrations, where the heat capacity of the solution differs greatly from that of the pure solvent, each solution acted as reference for the next as discussed in ref. 15. For the density measurements, *n*-heptane or *n*-octane and the alcohol were used as references.

From the experimentally obtained molar heat capacities, the excess molar heat capacities throughout the concentration range, C_p^E, and the dilute alcohol (component 1) apparent molar heat capacities, C_m^{app}, were calculated. C_m^{app} was obtained using

$$C_m^{app} = \frac{C_{m,\,soln} - x_2\,C_{m,\,2}}{x_1} \quad (1)$$

where $C_{m,\,soln}$ is the molar heat capacity of the solution and $C_{m,\,2}$ and x_2 are the molar heat capacity and mole fraction of the solvent. The C_p^E data was represented by the Redlich–Kister equation

$$C_p^E = x_1 x_2 \sum_i A_i (x_1 - x_2)^{i-1} \quad (2)$$

or, for highly asymmetric C_p^E, using the SSF equation[16]

$$C_p^E = \sum_i \frac{A_{2i-1} x_1 x_2}{(x_1 + A_{2i} x_2)^2} \quad (3)$$

For all the mixtures studied in this work, the A_i parameters are given in Table 1. In obtaining the A_i parameters, only the data measured in the experiment designed to obtain C_p^E throughout the concentration range were employed; typically, these experiments included at least three alcohol mole fractions below 0.1. The heat capacities for these solutions were found to be in excellent agreement with those obtained in the experiment designed to study the dilute alcohol region. Using the measured densities the alcohol apparent molar volumes, V_m^{app}, and excess molar volumes, V^E, can also be calculated. These data will be reported and discussed in a forthcoming article.[17]

Pure component, C_m^{app} and C_p^E data have been deposited as Supplementary Data.‡ Through repetition of the present systems, the accuracy appears to be $\pm 5 \times 10^{-6}$ g cm^{-3} for the density, ± 5 J K^{-1} mol^{-1} for C_m^{app} and its infinite dilution limit, and ± 0.2 J K^{-1} mol^{-1} for C_p^E.

‡ Supplementary material (**SUP 57478**, 12 pp.) deposited with the British Library. Details are available from the Editorial Office. For direct electronic access see http://www.rsc.org/suppdata/cp/1999/665.

Results and discussion

Apparent molar heat capacities

The experimental results for the apparent molar heat capacity C_m^{app} for ethanol and decan-1-ol in the inert *n*-octane and the unsaturated hydrocarbons oct-1-ene and oct-1-yne, calculated using eqn. (1), are shown in Fig. 1. For all the other alkan-1-ols reported in this work, the general features shown in Fig. 1 are the same, *i.e.*, C_m^{app} shows a large maximum at low alcohol concentrations. The magnitude of this effect can be appreciated from the difference between the maximum in C_m^{app} and the heat capacity of the pure alcohol. For example, for ethanol in *n*-octane and oct-1-yne these differences are *ca.* 260 and 110 J K^{-1} mol^{-1}, respectively, which are more than twice (*n*-octane) and of the same magnitude (oct-1-yne) as the heat capacity of the pure alcohol itself (*ca.* 110 J K^{-1} mol^{-1}). The very large maxima for ethanol and decan-1-ol in *n*-octane are a reflection of the high degree of structure or organization,[1–4] produced by the formation of multimers, *i.e.*, self-association *via* H-bonding, that takes place at very dilute alcohol concentrations. The infinite-dilution apparent molar heat capacity for ethanol + *n*-octane and decan-1-ol + *n*-octane in Fig. 1 represent the contribution to the heat capacity of the alcohol in the absence of any association, each alcohol molecule being isolated in the inert solvent. Thus for all the mixtures studied here, the associational part of the apparent molar heat capacity, $C_{m,\,assoc}^{app}$, is given by

$$C_{m,\,assoc}^{app} = C_m^{app} - C_m^{app,\,in}(x_1 \rightarrow 0) \qquad (4)$$

where $C_m^{app,\,in}(x_1 \rightarrow 0)$ is the infinite-dilution limit of C_m^{app} in the alcohol + inert solvent (*n*-octane) mixture; it is thus assumed that the physical contributions to C_m^{app}, *i.e.*, those arising from interactions other than the association itself do not change with alcohol concentration. This assumption is reasonable as indicated by the small C_p^E in most non-electrolyte mixtures.

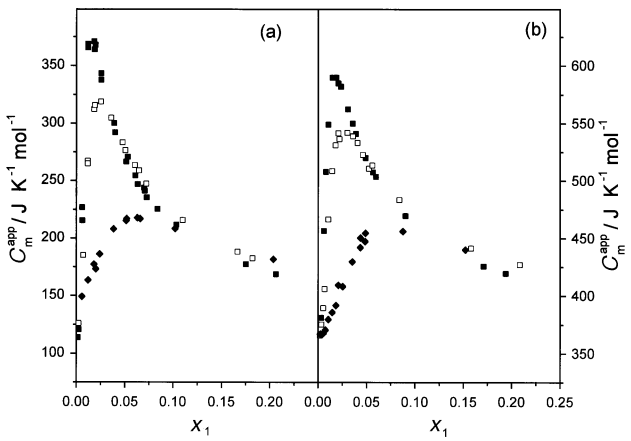

Fig. 1 Apparent molar heat C_m^{app} at 25 °C for (a) ethanol (1) in *n*-octane (■), oct-1-ene (□) and oct-1-yne (◆) and for (b) decan-1-ol (1) in *n*-octane (■), oct-1-ene (□) and oct-1-yne (◆).

Table 2 shows $C_m^{app,\,in}(x_1 \rightarrow 0)$ for all the alkan-1-ols in *n*-octane and the infinite-dilution apparent molar heat capacities, $C_m^{app}(x_1 \rightarrow 0)$ of the alcohols in the other solvents used. These values were obtained from extrapolation of data as that shown in Fig. 1. From eqn. (4), the infinite-dilution value of $C_{m,\,assoc}^{app}$ is

$$C_{m,\,assoc}^{app}(x_1 \rightarrow 0) = C_m^{app}(x_1 \rightarrow 0) - C_m^{app,\,in}(x_1 \rightarrow 0) \qquad (5)$$

and hence for an alcohol in an inert solvent $C_{m,\,assoc}^{app}(x_1 \rightarrow 0) = 0$, while for an alcohol in a non-inert solvent this limiting value is different from zero. From Table 2, the average $C_{m,\,assoc}^{app}(x_1 \rightarrow 0)$ are 21 and 28 J K^{-1} mol^{-1} for alkam-1-ols in oct-1-ene and oct-1-yne, respectively, indicating that the alcohol molecules at infinite dilution in these unsaturated hydrocarbons are associated with the solvent.

Using eqn. (4) and the values in Table 2, the associational part of the apparent molar heat capacities of propan-1-ol and hexan-1-ol in *n*-octane, oct-1-ene and oct-1-yne are shown in Fig. 2. In the inert *n*-octane, as the alcohol concentration increases $C_{m,\,assoc}^{app}$ increases rapidly corresponding to the formation of structure caused by the coming together of alcohol molecules over long distances to form multimers. With further increase in concentration $C_{m,\,assoc}^{app}$ decreases because alcohol molecules must come together to form multimers over shorter distances, *i.e.*, the entropy decrease produced by the formation of a multimer is, at these concentrations, smaller than that occurring in the more dilute region. Characteristic changes in $C_{m,\,assoc}^{app}$ occur when the environment changes from the inert *n*-octane to the unsaturated oct-1-ene and oct-1-yne. Fig. 2 indicates that for both alcohols the magnitude of the maximum in $C_{m,\,assoc}^{app}$ is reduced and displaced to higher alcohol concentrations, the effect being more pronounced for oct-1-yne. The interference of oct-1-ene and oct-1-yne in the

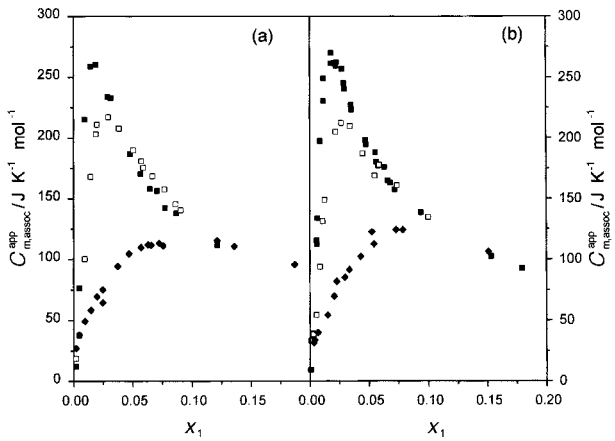

Fig. 2 Associational part of the apparent molar heat capacity $C_{m,\,assoc}^{app}$ at 25 °C for (a) propan-1-ol (1) in *n*-octane (■), oct-1-ene (□) and oct-1-yne (◆) and for (b) hexan-1-ol (1) in *n*-octane (■), oct-1-ene (□) and oct-1-yne (◆). Although not visible owing to the scale, at zero alcohol concentration $C_{m,\,assoc}^{app} = 21$ and 28 J K^{-1} mol^{-1} in oct-1-ene and oct-1-yne, respectively.

Table 2 Infinite-dilution apparent molar heat capacities (in J K^{-1} mol^{-1}) at 25 °C for alkan-1-ols in an inert solvent (*n*-octane or cyclohexane), $C_m^{app,\,in}(x_1 \rightarrow 0)$ and in several unsaturated hydrocarbons $C_m^{app}(x_1 \rightarrow 0)$

	Methanol	Ethanol	Propan-1-ol	Hexan-1-ol	Decan-1-ol
n-Octane[a]	72	100	130	215	338
Oct-1-ene	100	120	145	235	360
Oct-1-yne	105	130	150	247	365
Oct-4-yne				250	
Hex-1-ene				222	
Cyclohexane				215	
Cyclohexene				227	
Benzene				218	

[a] From ref. 2 except for propan-1-ol (this work).

self-association of alkan-1-ols is reminiscent of that seen when a proton acceptor is added to an alcohol–hydrocarbon mixture. In ref. 8 $C^{app}_{m,assoc}$ was measured as a function of alcohol concentration for ternary solutions of the type hexan-1-ol + (methyl acetate + *n*-dodecane); there, as the concentration of methyl acetate (MA) increased, the maximum in $C^{app}_{m,assoc}$ decreased and moved to higher hexan-1-ol concentrations, *i.e.*, a behaviour analogous to that seen in Fig. 2. The decrease and displacement of $C^{app}_{m,assoc}$ was shown to be due to the formation of a 1 : 1 complex between MA and hexan-1-ol, *i.e.*, to the formation of a H-bond between the carbonyl group in MA and the hydroxy group in the alkan-1-ol. The formation of this new species in solution competes with the formation of self-associated species and as a result $C^{app}_{m,assoc}$ decreases. This competition can be "tuned" by changing the amount of proton acceptor used in the ternary mixture. In this work, we have measured $C^{app}_{m,assoc}$ for the ternary solution hexan-1-ol + (oct-1-yne + *n*-octane) with oct-1-yne and *n*-octane being at equimolar concentration. Fig. 3 compares $C^{app}_{m,assoc}$ for hexan-1-ol in the binary oct-1-yne + *n*-octane with the results in *n*-octane and in oct-1-yne. Clearly, the decrease in $C^{app}_{m,assoc}$ in going from the *n*-octane case to the ternary mixture is due to the presence of oct-1-yne, which interferes with the alcohol self-association forming a complex with hexan-1-ol. It is concluded that both oct-1-ene and oct-1-yne act as weak proton acceptors, forming complexes or cross-associated species with the alcohol molecules. From the $C^{app}_{m,assoc}$ results in Fig. 2, it appears that (i) the alcohol–alkene complexes are energetically weaker than the alcohol–alkyne ones and (ii) there are more alcohol self-associated species and fewer alcohol–unsaturated hydrocarbon complexes in oct-1-ene than in oct-1-yne.

The effects seen in Fig. 1 to 3 are not exclusive of linear unsaturated hydrocarbons. Fig. 4 displays $C^{app}_{m,assoc}$ for hexan-1-ol in the inert cyclohexane, and the unsaturated cyclic hydrocarbons cyclohexene and benzene. As expected, in Table 2 cyclohexane is seen to behave as the inert *n*-octane, while $C^{app}_{m,assoc}(x_1 \rightarrow 0)$ for cyclohexene and benzene are positive but small. In Fig. 4, $C^{app}_{m,assoc}$ for 1-hexanol decreases in going from cyclohexane to cyclohexene, a drop which is comparable to that seen in Fig. 2 for oct-1-ene. A further reduction in $C^{app}_{m,assoc}$ values is observed when benzene is the solvent, this decrease being similar to that obtained for oct-1-yne in Fig. 2; hence, it appears benzene forms a complex with hexan-1-ol which is similar (in strength and in its effect over the alcohol self-association) than that formed between hexan-1-ol and oct-1-yne. The results in Fig. 4 and 2 also show that the behaviour of $C^{app}_{m,assoc}$ does not depend significantly on the molecular geometry of the unsaturated hydrocarbon, but rather on the solvent capacity to associate with the alcohol.

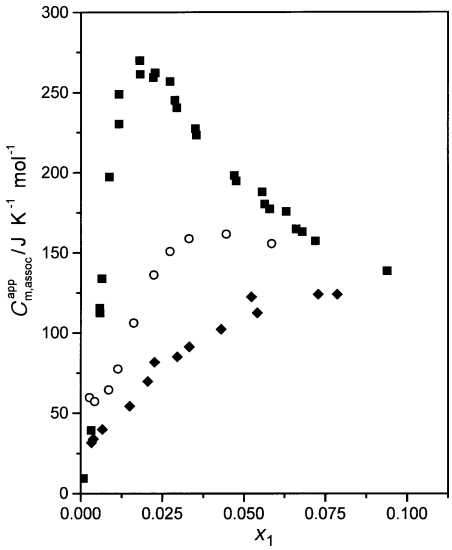

Fig. 3 Associational part of the apparent molar heat capacity $C^{app}_{m,assoc}$ at 25 °C for hexan-1-ol in *n*-octane (■), oct-1-yne (◆) and an equimolar mixture of *n*-octane and oct-1-yne (○) against hexan-1-ol mole fraction.

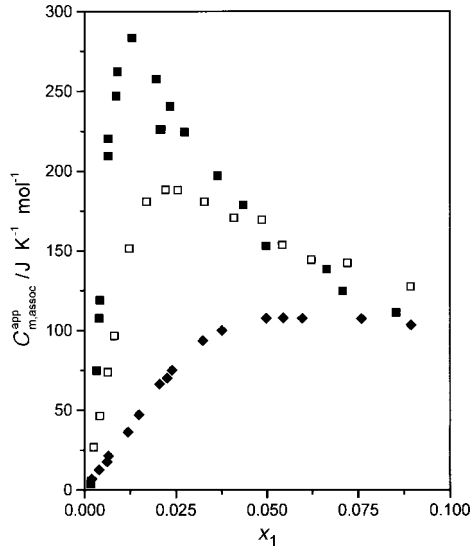

Fig. 4 Associational part of the apparent molar heat capacity $C^{app}_{m,assoc}$ at 25 °C for hexan-1-ol in cyclohexane (■), cyclohexene (□) and in benzene (◆) against hexan-1-ol mole fraction.

Corresponding states

When alkan-1-ol $C^{app}_{m,assoc}$ values in inert solvents are plotted against alcohol concentration expressed as volume fraction, or weight fraction or mole fraction, a spread of curves is found;[2] a similar situation is encountered for all the $C^{app}_{m,assoc}$ values obtained in this work. This behaviour has its roots in the fact that these concentration variables refer to alcohol molecules rather than to hydroxy groups. A more convenient concentration variable, originally introduced by Pouchly,[18] is ψ_1 which is the number of moles of alcohol per mole of segments in the system. As such, ψ_1 is

$$\psi_1 = x_1/(x_1 r_1 + x_2 r_2) \quad (6)$$

where r_1 and r_2 are the number of segments in the alcohol and the solvent defined by dividing the molar volumes by the molar segmental volume *v*. ψ_1 can then be considered as the concentration of hydroxy groups rather than alcohol molecules in the solution. The advantage of using ψ_1 as concentration variable was demonstrated in ref. 2 where it was shown that dilute range $C^{app}_{m,assoc}$ data for all alkan-1-ols (a total of 236 experimental points) in any inert solvent (*n*-alkanes) follow a corresponding states behaviour, *i.e.*, a plot of $C^{app}_{m,assoc}$ *vs.* ψ_1 is a unique curve for all alkan-1-ols in all inert solvents. This corresponding states behaviour has also been found recently[5] for 1,2-diols in the inert *n*-heptane (83 experimental points) and in the non-inert carbon tetrachloride (93 experimental points). Fig. 5 shows the alkan-1-ol $C^{app}_{m,assoc}$ values measured in this work plotted against ψ_1. Here, we have used the molar volume of methanol (40.7 cm^3 mol^{-1}), the smallest possible alkan-1-ol, as the value for *v*. It is clearly seen in Fig. 5 that for each of the three solvents, all the alkan-1-ol $C^{app}_{m,assoc}$ values collapse into a single or corresponding states curve providing a striking demonstration of the fact that the ordering of alkan-1-ol molecules in solution (self-association alone or together with cross-association with the non-inert solvent) depends on the concentration of hydroxy groups, independently of the alcohol chain length. From the collapse[2] of $C^{app}_{m,assoc}$ values for many alkan-1-ols in many different *n*-alkanes into a single curve, it is possible to speculate

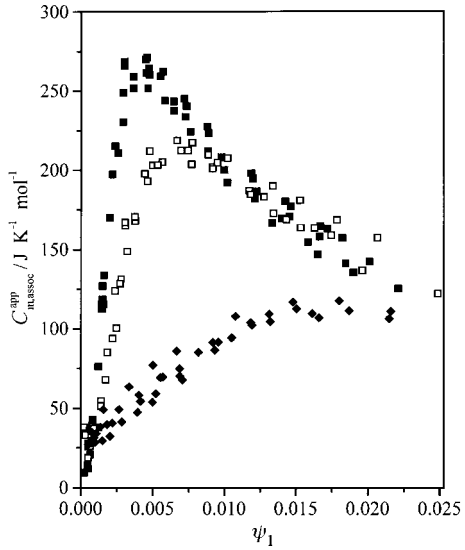

Fig. 5 Associational part of the apparent molar heat capacity $C^{app}_{m,assoc}$ at 25 °C against ψ_1 for alkan-1-ols in *n*-octane (■), oct-1-ene (□) and oct-1-yne (◆). The number of experimental points are 63 for *n*-octane, 55 for oct-1-ene and 45 for oct-1-yne. Although not visible owing to the scale, at zero alcohol concentration $C^{app}_{m,assoc} = 21$ and 28 J K^{-1} mol^{-1} in oct-1-ene and oct-1-yne, respectively.

that $C^{app}_{m,assoc}$ will also be independent of the solvent chain length of alk-1-enes and alk-1-ynes. The fact that for all alkan-1-ol a unique $C^{app}_{m,assoc}$ *vs.* ψ_1 curve is obtained, indicates that their self-association and complex formation with alk-1-enes and alk-1-ynes, can be described with a single set of parameters, one set for each solvent used. This can be achieved, as discussed below, using the TK model.

Application of the TK model

The TK model and its application to the study of self-association of alcohols in inert solvents has been discussed in detail in ref. 1–4. This model was extended to consider the case where complex formation or cross association between the two components is also present in solution.[6, 8] In this case, the associational part of the apparent molar heat capacity of the alcohol is given by (eqn. (1) in ref. 6 or eqn. (1) in ref. 8)

$$C^{app}_{m,assoc} = \left\{\left(\frac{\Delta H^\circ}{T}\right)^2 \frac{1}{R}\left\{\sum_{i=2}\frac{i-1}{i}K_i\frac{\phi_A^i}{\phi_1} \times\left[(i-1)\left(\frac{\phi_2 X}{r}+1\right)+\sum_{j\neq i}(i-j)K_j\phi_A^{j-1}\right]\right\} - \frac{\Delta H^\circ \Delta H^\circ_{11}}{RT^2}\left(\frac{2\phi_2 X}{r\phi_1}\sum_{i=2}(i-1)K_i\phi_A^i\right) + \left(\frac{\Delta H^\circ_{11}}{T}\right)^2\frac{1}{R}\left[\frac{\phi_2 X}{r\phi_1}\left(\phi_A+\sum_{i=2}iK_i\phi_A^i\right)\right]\right\} \Big/ \left(1+\sum_{j=2}jK_j\phi_A^{j-1}+\frac{\phi_2 X}{r}\right) \quad (7)$$

where

$$X = \frac{\frac{r}{r+1}K_{11}}{\left[\frac{r}{r+1}K_{11}\phi_A+1\right]^2} \quad \text{and} \quad \phi_1 = \frac{x_1}{x_1+rx_2} \quad (8)$$

Note that in ref. 8 there is an error in the sign of the second term of eqn. (7). In obtaining eqn. (7) only the 1 : 1 cross-associated species has been considered, so that K_{11} and ΔH°_{11} are the volumetric equilibrium constant and the enthalpy change for the formation of this 1 : 1 species and r is the ratio of molar volumes V_2/V_1 (component 1 being the alcohol). ΔH° represents the self-association enthalpy change corresponding to the formation of a mole of H-bonds, K_i are the volumetric equilibrium constants for every self-associated species i or i-mer in solution, ϕ_1 is the alcohol volume fraction in solution and ϕ_A is the volume fraction of alcohol which is in the form of monomers. This fraction is obtained as the closest root to zero of the mass balance equation

$$\sum_{i=2}\phi_A^i K_i + \phi_A + \frac{\phi_2}{r}\frac{\frac{r}{1+r}K_{11}\phi_A}{\frac{r}{1+r}K_{11}\phi_A+1} - \phi_1 = 0 \quad (9)$$

which can be easily found using the Newton–Raphson numerical method. The first term in eqn. (7) represents the associational part of the apparent molar heat capacity of the alcohol due to the self-association process (in the presence of complex formation), the third corresponds to the formation of the 1 : 1 complex (in the presence of self-association) and the second is a cross-term. In eqn. (7), only the so called "chemical contributions" to the heat capacity, *i.e.*, those arising from the association or dissociation processes have been considered, the "physical contributions" due to interactions in the system other than the association itself, being ignored. Given that heat capacity is mainly a reflection of the chemical contributions in the mixture, the TK model is a good tool to obtain valuable information on the microscopic behaviour of mixtures where association–dissociation equilibria are present. On the other hand, ignoring the physical contributions makes the TK model inadequate to correlate or fully analyze apparent or excess thermodynamic properties where these contributions are important, *e.g.* H^E or H^{app}_m and V^E or V^{app}_m. Using the TK model in these cases can only produce a rough estimation of the chemical contributions to H^E (the chemical contribution to V^E is assumed to be zero in the TK model).

The TK model expression for $C^{app}_{m,assoc}$, *i.e.*, eqn. (7), contains several parameters *viz.*, ΔH°_{11}, ΔH°, K_{11} and the equilibrium constants K_i. ΔH° and the K_i refer to the alcohol self-association in solution and hence they should be obtained from data on mixtures where only self-association equilibria are present, *i.e.*, data for mixtures of alcohols with inert (*n*-alkane) solvents. This has already been done in ref. 2 and hence ΔH° and the K_i are known for all the alkan-1-ols used here, with the exception of ethanol (re-measured in this work) and propan-1-ol whose parameters were obtained here. Furthermore, in ref. 1 and 2 it was found that to explain $C^{app}_{m,assoc}$ data for alkan-1-ols + *n*-alkanes, it is enough to consider only one multimer, *viz.*, either linear or cyclic tetramers (K_4). The two remaining parameters, ΔH°_{11} and K_{11}, were fitted in the least square sense to the $C^{app}_{m,assoc}$ data for oct-1-ene and oct-1-yne. This fitting produced ΔH°_{11} values which were very similar for all alkan-1-ols in a given solvent; hence, the parameter K_{11} was fitted again, this time using the average ΔH°_{11} value as constant. Table 3 reports these fitted ΔH°_{11} and K_{11} values, together with the ΔH° and K_4 values for alcohol self-association. The K_4 values are orders or magnitude bigger than the K_{11} values, reflecting the dominance of self-associated species in the solution. The ΔH°_{11} values in Table 3 indicate that the alkan-1-ol–oct-1-ene complex is weaker than the alkan-1-ol–oct-1-yne complex; for all alkan-1-ols the equilibrium constant K_{11} is bigger for oct-1-yne than for oct-1-ene, indicating that there are more 1 : 1 complexes formed in the alkyne. Both these conclusions are in agreement with the previously presented qualitative discussion of the data. The quality of the fit achieved using eqn. (7) is exemplified in Fig. 6 for the cases of methanol and propan-1-ol, the fit

Table 3 Volumetric equilibrium constant for the formation of tetramers K_4, enthalpy change ΔH° for the formation of a H-bond (kJ mol^{-1}), volumetric equilibrium constant K_{11} and enthalpy change ΔH°_{11} (kJ mol^{-1}) for the formation of the alcohol–unsaturated hydrocarbon complex at 25 °C for alkan-1-ols in the inert *n*-octane, in oct-1-ene and in oct-1-yne

	n-Octane		Oct-1-ene		Oct-1-yne	
	ΔH° [a]	K_4 [a]	ΔH°_{11}	K_{11}	ΔH°_{11}	K_{11}
Methanol	27.9	31.39×10^6	9.6	2.24	12.7	14.04
Ethanol	28.1	8.71×10^6	9.6	1.45	12.7	8.07
Propan-1-ol	28.1	3.42×10^6	9.6	1.47	12.7	7.98
Hexan-1-ol	28.4	6.9×10^5	9.6	1.06	12.7	5.48
Decan-1-ol	28.1	2.4×10^5	9.6	0.94	12.7	4.80

[a] From ref. 2 except for ethanol and propan-1-ol (this work).

for the other three alcohols being similar. When $C^{app}_{m,assoc}$ data for hexan-1-ol + oct-4-yne are fitted, the obtained K_{11} and ΔH°_{11} values are very close to that for oct-1-yne (4.41 *vs.* 5.48 and 13.8 kJ mol^{-1} *vs.* 12.7 kJ mol^{-1}, respectively), implying that the alcohol–alkyne interaction is mainly between the hydroxy group in the alcohol and the triple bond in the alkyne. The fitted K_{11} and ΔH°_{11} values for hexan-1-ol mixed with cyclohexene (1.52 and 9.5 kJ mol^{-1}) and benzene (6.08 and 11.4 kJ mol^{-1}) are close to the respective values for oct-1-ene and oct-1-yne (see Table 3), corroborating that cyclohexene behaves as a linear unsaturated hydrocarbon and that the alcohol–benzene complex is similar to the alcohol–alkyne one.

The volumetric equilibrium constants K_{11} in Table 3 for the different alcohols interacting with oct-1-ene and with oct-1-yne depend on the size of the molecules involved. This dependence is shown in Fig. 7a and b. These volumetric equilibrium constants can be transformed into a unique more fundamental or intrinsic equilibrium constant K^{int}_{11}, which is independent of molecular size and describes the association between the hydroxy group in the alcohol and the double and triple bond in oct-1-ene and oct-1-yne, respectively. A similar transformation has been done for alcohol–ester and alcohol–AOT reverse micelles interactions.[7,9] The transformation can be achieved[2,7] using the Flory lattice theory giving

$$K_{11} = K^{int}_{11}(r_1^{-1} + r_2^{-1})\,\frac{\omega^2\sigma_1\sigma_2}{z\sigma_{12}} \qquad (10)$$

where r_1 and r_2 were defined in regard to eqn. (6). In eqn. (10), ω is the flexibility parameter for the complex and z is the lattice coordination number, taken as in ref. 2 to be 1.69 and

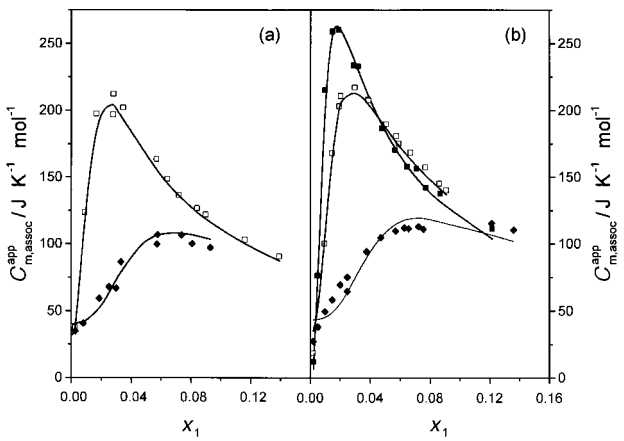

Fig. 6 Associational part of the apparent molar heat capacity $C^{app}_{m,assoc}$ at 25 °C for (a) methanol (1) in oct-1-ene (□) and oct-1-yne (◆) and for (b) propan-1-ol (1) in *n*-octane (■), oct-1-ene (□) and oct-1-yne (◆). The solid lines are the best fit obtained using the TK model (parameters in Table 3).

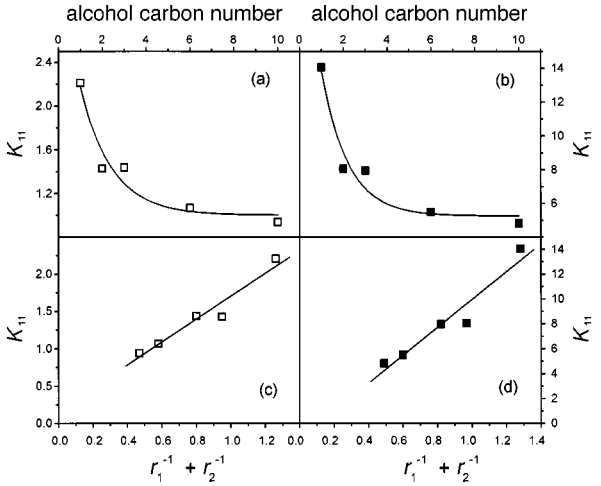

Fig. 7 Volumetric equilibrium constants K_{11} against alcohol carbon number in oct-1-ene (a) and in oct-1-yne (b), and against $(r_1^{-1} + r_2^{-1})$ for oct-1-ene (c) and oct-1-yne (d). In (a) and (b) curves are only to aid visualization. In (c) and (d) the straight lines are a fit to the K_{11} data according to eqn. (10).

10, respectively; σ_1 and σ_2 are symmetry numbers for the alcohol and unsaturated hydrocarbon molecules taken equal to 2, but $\sigma_{12} = 1$, reflecting the asymmetry of the complex. Eqn. (10) then translates the intermolecular K_{11} into the intergroup equilibrium constant K^{int}_{11} through the molecular chain lengths r_1 and r_2, reflecting the entropy lowering involved in localizing the hydroxy group (OH) in the alcohol and the double or triple bond in oct-1-ene and oct-1-yne, to form an OH–double bond or OH–triple bond interaction. According to eqn. (10), a plot of the volumetric equilibrium constants K_{11} against $(r_1^{-1} + r_2^{-1})$ should be a straight line with zero intercept, the slope providing the K^{int}_{11} value. This is tested in Fig. 7c and d where the data are seen to be well fitted by straight lines (correlation coefficients of 0.973 and 0.965 for oct-1-ene and oct-1-yne, respectively) with intercepts of 0.15 (oct-1-ene) and −1.29 (oct-1-yne) and slopes of 1.58 (oct-1-ene) and 11.25 (oct-1-yne). From these slopes and the values for the several parameters in the Flory lattice theory the thermodynamic parameters characterizing the 1-alcohol–alkene complex are at 25 °C

$$\begin{aligned} K^{int}_{11} &= 1.38 \pm 0.20 \\ \Delta G^\circ_{11} &= -0.80 \pm 0.4 \text{ kJ mol}^{-1} \\ \Delta H^\circ_{11} &= -9.6 \pm 0.5 \text{ kJ mol}^{-1} \\ \Delta S^\circ_{11} &= -29.5 \pm 1.0 \text{ J K}^{-1} \text{ mol}^{-1} \end{aligned} \qquad (11)$$

and for the 1-alcohol–alkyne complex

$$\begin{aligned} K^{int}_{11} &= 9.85 \pm 1.5 \\ \Delta G^\circ_{11} &= -5.66 \pm 0.40 \text{ kJ mol}^{-1} \\ \Delta H^\circ_{11} &= -12.7 \pm 0.5 \text{ kJ mol}^{-1} \\ \Delta S^\circ_{11} &= -23.6 \pm 1.0 \text{ J K}^{-1} \text{ mol}^{-1} \end{aligned} \qquad (12)$$

From the ΔG°_{11} (or K^{int}_{11}) values in eqn. (11) and (12), it is clear that the formation of alkan-1-ol–alkene complexes is less favourable than the formation of alkan-1-ol–alkyne complexes; in fact, the alkan-1-ol–alkene complex is only marginally stable and this might be the reason for these complexes not being evident in the V^E and H^E results in ref. 10–14. It is also interesting to compare the thermodynamic values in eqn. (11) and (12) with those obtained previously for (i) alkan-1-ol–ester (the OH–COO chemical groups interaction)[7] where $\Delta G^\circ_{11} = -10$ kJ mol^{-1} and $\Delta H^\circ_{11} = -20$ kJ mol^{-1} and for (ii) alkan-1-ol–ionic head of the AOT surfactant[9] where $\Delta G^\circ_{11} = -15.1$ kJ mol^{-1} and $\Delta H^\circ_{11} = -25$ kJ mol^{-1}; this comparison shows that, as expected, the association between alcohol molecules

and double or triple bonds are much weaker than those formed with the lone electron pairs in the COO group or with ionic entities. All these results confirm the sensitivity of heat capacity as a good sensor for structure creation or destruction in solution.[19] At the present time, this sensitivity is being used to study complexes formed between aromatic molecules as well as the formation of NH–π and CH–π complexes.[20]

For alkan-1-ol self-association, the volumetric equilibrium constants K_4 for tetramer formation in Table 3 can be also transformed into a unique constant K_4^{int}; this was done in ref. 2 (for linear tetramers) using an average enthalpy change for H-bond formation (from eight alkan-1-ols) giving at 25 °C

$$K_4^{int} = 328 \pm 30$$
$$\Delta G_4^\circ = -14.4 \pm 0.3 \text{ kJ mol}^{-1}$$
$$\Delta H_4^\circ = -28.3 \pm 0.6 \text{ kJ mol}^{-1}$$
$$\Delta S_4^\circ = -46.6 \pm 1.0 \text{ J K}^{-1} \text{ mol}^{-1} \quad (13)$$

The above set of parameters completely characterize the apparent molar heat capacities at dilute alcohol concentrations for all alkan-1-ol + inert *n*-alkane mixtures (eqn. (13)), for all alkan-1-ol + alkene mixtures (eqn. (11) and 13)) and for all alkan-1-ol + alkyne mixtures (eqn. (12) and (13)). They express, within the framework of the TK model, the experimental finding that $C_{m,\,assoc}^{app}$ data follows a corresponding states behaviour.

Excess heat capacities

The excess heat capacities, C_p^E, and $C_{m,\,assoc}^{app}$ are related by

$$C_p^E = x_1(C_m^{app} - C_{m,1}) = x_1(C_{m,\,assoc}^{app} - C_{m,1,\,assoc}) \quad (14)$$

where $C_{m,\,1,\,assoc}$ is the associational part of the molar heat capacity of the pure alcohol, *i.e.*, $C_{m,\,1,\,assoc} = C_{m,1} - C_m^{app,\,in}(x_1 \rightarrow 0)$ according to eqn. (4). C_p^E then involves a comparison between the degree of association of the alcohol in the solution and in the pure state. Fig. 8 and 9 show C_p^E for hexan-1-ol mixed with *n*-octane, oct-1-ene and oct-1-yne as a function of alcohol mole fraction both in the dilute concentration range and throughout the concentration interval; for the other alcohols, the C_p^E curves show analogous features. In the dilute alcohol region shown in Fig. 8 C_p^E (*n*-octane) > C_p^E (oct-1-ene) > C_p^E (oct-1-yne); this is a reflection of the high degree of structuring that the alcohol attains in the inert *n*-octane, as compared with that in oct-1-yne where the formation of alcohol–octyne complexes interferes with the formation of

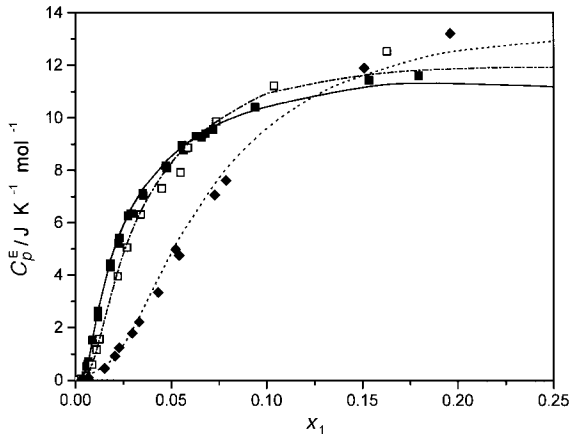

Fig. 8 Molar excess heat capacity C_p^E at 25 °C at low alcohol concentrations for hexan-1-ol (1) with *n*-octane (■), oct-1-ene (□) and oct-1-yne (◆). The TK model predictions were obtained using eqn. (7) and (14) for *n*-octane (full line), oct-1-ene (dot-dashed line) and oct-1-yne (dotted line).

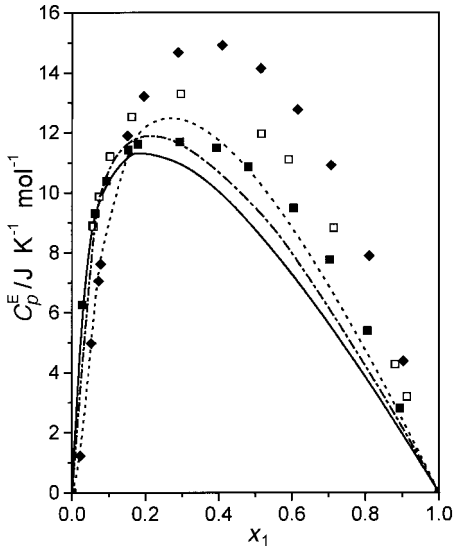

Fig. 9 Molar excess heat capacity C_p^E at 25 °C throughout the concentration range for hexan-1-ol (1) with *n*-octane (■), oct-1-ene (□) and oct-1-yne (◆). The TK model predictions were obtained using eqn. (7) and (14) for *n*-octane (full line), oct-1-ene (dot-dashed line) and oct-1-yne (dotted line).

alcohol self-associated species, *viz.*, tetramers, whose formation is delayed to higher concentrations. For all the alcohols studied, at alcohol mole fractions between 0.1 and 0.2 the C_p^E curves cross each other and the relation between them becomes C_p^E (*n*-octane) < C_p^E (oct-1-ene) < C_p^E (oct-1-yne). In Fig. 9, the maxima of the curves for oct-1-yne fall near equimolar concentration; this symmetry was also found for alcohol–proton acceptor (esters) systems in ref. 7 and is a reflection of the higher alcohol concentrations at which $C_{m,\,assoc}^{app}$ attains a maximum (see Fig. 1 and 2). The maxima of C_p^E for the alcohol mixed with oct-1-ene and *n*-octane are found at progressively lower alcohol concentrations. For the inert *n*-octane the C_p^E curve is markedly asymmetric, this being a general feature of all alcohol–inert systems as discussed in ref. 2.

Fig. 8 and 9 also show C_p^E calculated with the TK model using eqn. (14) and the parameters in Table 3. Here, for the pure alcohol $C_{m,1,\,assoc}$ was obtained from eqn. (7) at $x_1 = \phi_1 = 1$. In Fig. 8, although $C_{m,\,assoc}^{app}$ was fitted to the experimental data, the C_p^E calculation involves a predicted quantity, *viz.* $C_{m,1,\,assoc}$, and hence the TK curves can be considered as predictions. The same is true in Fig. 9, where the C_p^E curves are calculated in a concentration region different from that where the TK parameters were fitted (below the alcohol mole fraction of 0.2). Fig. 8 and 9 show that all the experimental trends, order of the C_p^E curves in both concentration regions, displacement of the maxima, *etc.*, are correctly predicted in a qualitative manner, showing that the TK model is a good tool to analyze heat capacity data. The TK interpretation of the C_p^E data is clarified by considering the associational energy, U_{assoc}, of an alcohol molecule in solution or in the pure state as given by the theory as a function of the temperature T. Fig. 10 gives results for an alcohol in the pure state and at a constant mole fraction in an active solvent (an alkene or an alkyne) and in the inert solvent; this is displayed at a low alcohol concentration in Fig. 10a and at a high alcohol concentration in Fig. 10b. At very low temperatures the alcohol molecules are in the lowest-energy state, corresponding to association in tetramers. With an increase of T, alcohol molecules move to the monomer energy level corresponding to complete breaking of the H-bonds. For the pure alcohol and for the alcohol in the inert solvent, direct dissociation of tetramers occurs. The rise in energy occurs at a lower T when the alcohol is diluted in the inert rather than in the pure liquid.

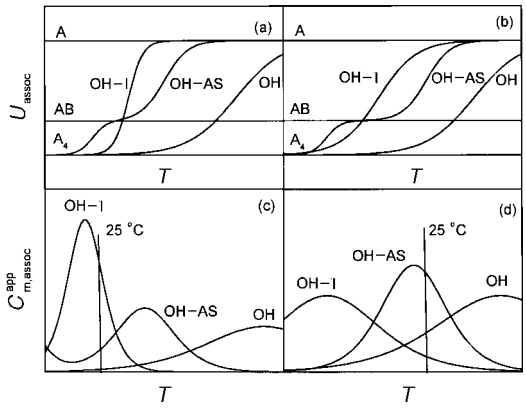

Fig. 10 Schematic representation of the associational energy U_{assoc} and apparent heat capacity $C^{app}_{m,assoc}$ against temperature T for: a pure alcohol (OH), a mixture of an alcohol and an inert hydrocarbon such as *n*-alkane (OH–I) and a mixture of an alcohol and an active solvent such as alkene or alkyne (OH–AS) at a low (*e.g.* 0.1 mol fraction) alcohol concentration [(a) and (c)] and at a higher (*e.g.* 0.5 mol fraction) alcohol concentration [(b) and (d)]. A, A_4 and **AB** represent the energy levels for alcohol monomers, tetramers and the 1 : 1 complex between the alcohol and the active solvent. According to (c), (d) and eqn. (14), at room temperature C^E_p (OH–I) > C^E_p (OH–AS) at low alcohol concentration and C^E_p (OH–I) < C^E_p (OH–AS) at a higher alcohol concentration.

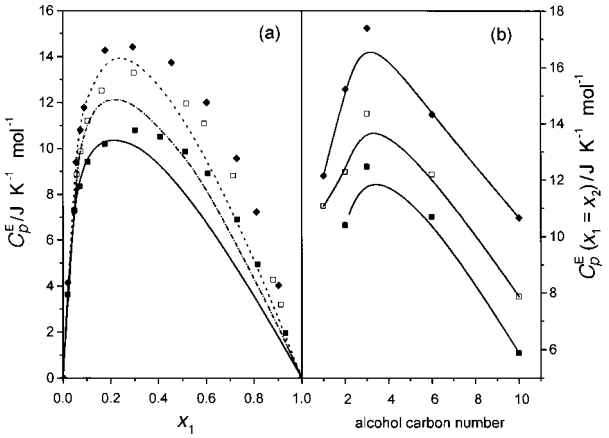

Fig. 11 (a) Molar excess heat capacity C^E_p at 25 °C for hexan-1-ol (1) with hex-1-ene (■), oct-1-ene (□) and dec-1-ene (◆). The TK model predictions were obtained using eqn. (7) and (14) for hex-1-ene (full line), oct-1-ene (dot-dashed line) and dec-1-ene (dotted line). In these predictions, the K_{11} and ΔK°_{11} parameters in Table 3 for oct-1-ene were employed for the other two alkenes (see text). (b) Experimental equimolar molar excess heat capacity C^E_p at 25 °C (from the RK or SSF representations of the data in Table 1) for all alkan-1-ols studied in this work mixed with *n*-octane (■), oct-1-ene (□) and oct-1-yne (◆). Lines are only to aid visualization.

However, for the alcohol in an alkene or alkyne, an intermediate energy level exists, *viz.* that of the complex, and the alcohol molecules remain complexed over a certain T range. With an increase in alcohol concentration, the energy *vs.* T curves are displaced towards the pure alcohol curve, the magnitude of this displacement depending on the values of the equilibrium constants involved, *i.e.*, on K_4 and K_{11}. The $C^{app}_{m,assoc}$ values correspond to the slopes of the energy curves against T, which are shown in Fig. 10c and 10d. It is clear that at 25 °C and low alcohol concentration (Fig. 10c) the alcohol $C^{app}_{m,assoc}$ is bigger in the inert solvent than in the active one producing, according to eqn. (14), a bigger C^E_p. When the alcohol concentration increases (Fig. 10d) this situation is reversed, *i.e.*, $C^{app}_{m,assoc}$ and hence C^E_p is bigger for the active solvent. The reason for the cross-over of the C^E_p curves seen in Fig. 8 and 9 is then that at high alcohol concentrations the alcohol–alkene or alcohol–alkyne complex dissociates at a higher temperature.

There are two other trends of the C^E_p data which are relevant. The first trend is shown in Fig. 11a, where the C^E_p for hexan-1-ol mixed with three alk-1-enes of different chain length are displayed; although not verified in this work, it is reasonable to assume that the trend observed in Fig. 11a will also be present for any other alkan-1-ol. The TK model predictions in Fig. 11a are in good agreement with experiment. Here, eqn. (14) was employed using the same K_{11} and ΔH°_{11} for the three alkenes (see Table 3), the only parameter changing from one mixture to another being the ratio of molar volumes r; the use of the same K_{11} and ΔH°_{11} for the three alkenes is justified by the fact that fitting the dilute hexan-1-ol + hex-1-ene $C^{app}_{m,assoc}$ data with a fixed value for ΔH°_{11} (9.6 kJ mol^{-1}, see Table 3) produced the same K_{11} value as in the oct-1-ene case (1.05 instead of 1.06). The increase in C^E_p as the alkene chain length increases can be explained by the TK model using an energy and heat capacity *vs.* T diagram analogous to that shown in Fig. 10, this time for the case of an alcohol at constant concentration mixed with active solvents of different sizes. This was done in ref. 7 to analyze alcohol + ester mixtures (see Fig. 10 in that reference) and the conclusion, applicable to the result in Fig. 11a, is that C^E_p increase with alkene size because for the longer alkene molecule the alcohol–alkene complex dissociates at a lower temperature. The second interesting trend of C^E_p data is shown in Fig. 11b, where the equimolar C^E_p are plotted against alcohol carbon number for the different hydrocarbons. It is observed that for the three hydrocarbons, C^E_p ($x_1 = x_2$) first increases and then decreases with alcohol chain length, the maximum value being for the mixtures involving propan-1-ol. The behaviour of 1-alcohols in *n*-octane was reported previously for *n*-heptane and *n*-dodecane in ref. 2; it is interesting that this behaviour persists, and even becomes more pronounced, when the solvent is an alkene or an alkyne. The TK model calculations using the parameters in Table 3 (not shown in Fig. 11b) indicate that the observed behaviour is qualitatively predicted but with C^E_p values which are smaller (see Fig. 9) and the maximum for propan-1-ol being much less pronounced. As discussed in ref. 2 in the context of the corresponding states (CS) behaviour of alkan-1-ol + alkane systems, an increase in the alcohol chain length m decreases ψ_1 for the alcohol in solution and in the pure state. Thus, both terms in eqn. (14) increase with m and the sign of the C^E_p change is not evident; however, it was found[2] that the increase of $C_{m,1,assoc}$ is larger than that of $C^{app}_{m,assoc}$ for the solution and hence C^E_p must decrease with m for any system obeying the CS behaviour. Hence, in ref. 2 it was concluded that methanol and ethanol have an anomalous behaviour, their low C^E_p values being a consequence of strong H-bonding. The analysis of the oct-1-ene and oct-1-yne cases in Fig. 11b is complicated by the presence of the cross-associated species, but it is possible to speculate that the drop in C^E_p values for ethanol and methanol have the same origin as that in the octane case.

C^E_p from the ERAS model

Using the extended real associated solution (ERAS) model, V^E and H^E data for similar alcohol–unsaturated hydrocarbon mixtures have been recently studied.[10–14] The common mixtures are methanol, ethanol and propan-1-ol mixed with oct-1-ene and with oct-1-yne. It is then interesting to evaluate the performance of the ERAS model, which includes both chemical and physical contributions, with the C^E_p data reported here. In the literature, the ERAS model parameters for many mixtures have not been fitted in the statistical sense to experimental data[21–23] but rather estimated to give an overall satisfactory rendering of the qualitative and quantitative features of the data; this was the case in ref. 14 for the alcohol–unsaturated hydrocarbon mixtures also studied here. In calculating C^E_p with the ERAS model an additional parameter

appears, namely dX_{AB}/dT which represents the change of the physical interactions with temperature. Fig. 12a shows the ERAS model predictions for propan-1-ol using the parameters in ref. 14 with $dX_{AB}/dT = 0$. It is seen that the predicted C_p^E are not close to the experimental values. Furthermore, under this approximation, the model fails to give the correct relative magnitudes of the C_p^E for the three hydrocarbons, predicting that at all alcohol concentrations C_p^E (oct-1-yne) < C_p^E (oct-1-ene) = C_p^E (*n*-octane) while experimentally this is only true at low alcohol concentrations; the prediction that C_p^E (oct-1-ene) = C_p^E (*n*-octane) results from the fact that in ref. 14 it was found that no alcohol–alkene association was necessary to describe the V^E and H^E data. The performance of the ERAS model for the mixtures with methanol and ethanol is the same as that seen in Fig. 12a. For the case of alcohol–*n*-alkane mixtures, the observation that the ERAS model is not able to reproduce C_p^E data has been reported before by Hofman and Casanova,[24] who also propose a modification to the model. If a dX_{AB}/dT value different from zero (but equal for the three hydrocarbons) is used, the predicted C_p^E are qualitatively better but their relative magnitudes remain incorrect. The results of the ERAS model can be improved if the dX_{AB}/dT parameter is allowed to take different values for each hydrocarbon. Usually, dX_{AB}/dT is fitted to $H^E(T)$ which are not available for the present mixtures. We have then fitted (in a statistical sense) dX_{AB}/dT to the experimental C_p^E data, the results being shown in Fig. 12b for the case of propan-1-ol + oct-1-yne. The fitted dX_{AB}/dT values are positive and increase considerably in going from *n*-octane (0.24 J K^{-1} cm^{-3}) to oct-1-ene (0.39 J K^{-1} cm^{-3}) to oct-1-yne (0.63 J K^{-1} cm^{-3}). In order to describe the experimental C_p^E for oct-1-ene and oct-1-yne, the model requires unrealistic large physical contributions with their maxima occurring at high alcohol concentrations. This is illustrated in Fig. 12b where the two contributions to the total C_p^E are shown for propan-1-ol + oct-1-yne, and it is seen that the physical contribution turns out to be more than double the chemical one. For methanol and ethanol, similar increments of the fitted dX_{AB}/dT values in going from *n*-octane to oct-1-yne were found, producing again physical contributions for oct-1-yne that are larger or comparable to the chemical contributions. The results in Fig. 12b are indicative of model failures that hinder the use of the model as a predictive tool. This deficiency is not exclusive to the ERAS model but rather general, since it is also present in many other association models.

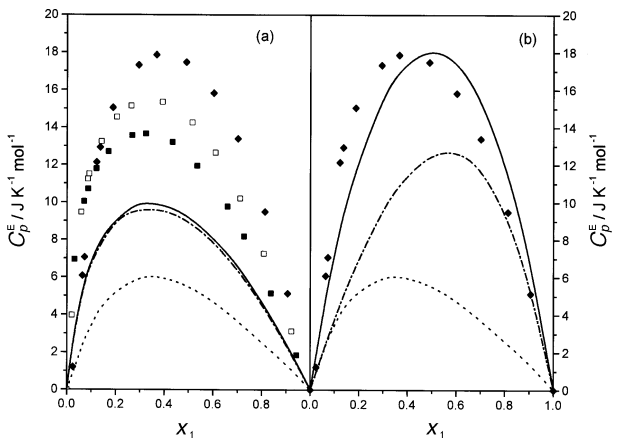

Fig. 12 (a) Molar excess heat capacity C_p^E at 25 °C for propan-1-ol (1) with *n*-octane (■), oct-1-ene (□) and oct-1-yne (◆). The ERAS model predictions were obtained using $dX_{AB}/dT = 0$ for *n* = octane (full line), oct-1-ene (dot–dashed line) and oct-1-yne (dotted line). (b) Molar excess heat capacity C_p^E at 25 °C for propan-1-ol (1) with oct-1-yne (◆). Here, the ERAS model $dX_{AB}/dT = 0.63$ J K^{-1} cm^{-3} parameter was fitted to the C_p^E data. The physical (dot–dashed line) and chemical (dotted line) contributions to the total C_p^E (full line) are shown.

The nature of the alcohol–unsaturated hydrocarbon interactions

For terminal and non-terminal alkenes and alkynes, *i.e.*, those with the double or triple bond positioned in the first carbon atom of the hydrocarbon chain or away from it, respectively, the possible interactions giving rise to the alcohol–unsaturated hydrocarbon complex are (i) between the proton of the hydroxy group of the alcohol and the negative electron density in the double or triple bond, producing what can be termed a H-bond, and (ii) between the lone pair electrons of the oxygen atom in the hydroxy group and the carbon atoms in the alkene or alkyne participating in the double or triple bond, an interaction that has been termed n–π interaction.[25,26] The existence of H-bonds between acidic hydrogens and regions of negative electron density has been experimentally shown for the case of benzene + water, using ground-state microwave spectroscopy.[27] The n–π interactions have been found to be important in explaining the H^E values of several alkenes mixed with carbon tetrachloride.[25,26] Terminal alkynes have been shown to have both proton accepting[28,29] and proton donating[28,30–34] abilities and hence a third interaction is possible in this case, namely (iii) a H-bond between the acid proton in the terminal alkyne and the oxygen of the hydroxy group of the alcohol; this is the interaction that was proposed to be present in ref. 14. All these interactions might be in competition and in this sense, the ΔH_{11}° and K_{11} values in Table 3 represent the total averaged interaction between alcohol and unsaturated hydrocarbon molecules. Note that if (iii) were to be the only interaction present, experiments with alcohols + non-terminal alkynes should not show any evidence of complex formation; on the other hand, interactions (i) and (ii) coexist but since the carbon atoms participating in the triple bond are not very electrophilic, interaction (i) must be considerably stronger and hence dominant over interaction (ii). In this context, quantum mechanical calculations can be helpful to further understand the nature of the alcohol–unsaturated hydrocarbon interactions. In order to advance in elucidating the dominant alcohol–unsaturated hydrocarbon interaction, $C_{m,assoc}^{app}$ for hexan-1-ol in oct-4-yne was measured in the dilute alcohol region. The results are displayed in Fig. 13a together with those for oct-1-yne. The $C_{m,assoc}^{app}$ for hexan-1-ol in oct-4-yne clearly indicates that there is complex formation in this mixture. Fig. 13a also indicates that $C_{m,assoc}^{app}$ for both alkynes (and their infinite dilution limits, see Table 2) are close, but distinguishable within the experimental error. The proximity of the $C_{m,assoc}^{app}$ values for both alkynes clearly indicates that interaction (i) is dominant, interaction (iii) being only marginally present in the oct-1-yne case. Similarly, it is possible to propose that interaction (i) is also dominant for alcohol–

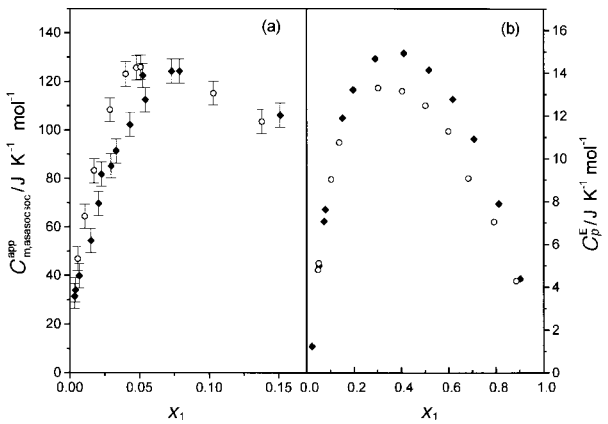

Fig. 13 Associational part of the apparent molar heat capacity $C_{m,assoc}^{app}$ (a) and molar excess heat capacity C_p^E (b) at 25 °C for hexan-1-ol in oct-1-yne (◆) and in oct-1-yne (○) against hexan-1-ol mole fraction. Bars in (a) are the estimated error.

alkene mixtures; given that the negative electron density of a double bond is smaller than that for a triple bond, the alcohol–alkyne complex must be stronger than the alcohol–alkene complex, in accordance with the results in Fig. 2. The presence of interaction (iii) for terminal alkynes is also revealed in the excess heat capacity data displayed in Fig. 13b where it is seen that C_p^E values are different in both alkynes; in fact, the C_p^E for hexan-1-ol + oct-4-yne is very close to that for hexan-1-ol mixed with the alkene oct-1-ene. The difference between the two C_p^E in Fig. 13b, *i.e.*, $\Delta C_p^E = C_p^E$ (oct-1-yne system) $- C_p^E$ (oct-4-yne system) $\cong 2$ J K^{-1} mol^{-1} at equimolar concentration, indicates that the contribution of interaction (iii) to the total complex formation interaction is rather small. Note that there is another possible explanation for the quantity ΔC_p^E not being zero, namely that all or part of the ΔC_p^E value in Fig. 13b is due to effect of molecular flexibility and shape connected with the more rigid oct-4-yne as compared with oct-1-yne. This effect has been shown to be present in C_p^E data for nonane isomers of varying degrees of rigidity mixed with *n*-octane,[35] the main finding in this regard being that with increasing flexibility C_p^E becomes more positive, as also seen in Fig. 13b. The effect of molecular rigidity or flexibility over the excess thermodynamic quantities has also been invoked in the analysis of H^E data for hex-1-yne and hex-3-yne mixed with inert and non-inert substances.[36,37] In summary, the alcohol–alkyne complex appears to be due to interaction (i) for non-terminal and terminal alkynes with a small contribution from interaction (iii) in the latter case; interaction (ii), if present, would be superimposed on the other two interactions and its small effect equally present in both types of alkynes. Similarly, interaction (i) must be dominant in the formation of alcohol–alkene complexes. These conclusions are consistent with those reached in ref. 37 where the acidic hydrogen of the terminal alkyne, *i.e.*, that intervening in interaction (iii), was found to be the determining factor explaining the differences in H^E values for terminal and non-terminal alkynes (hexynes) mixed with dipropyl ether (DPE) and triethylamine (TEA); for these mixtures, since there is no acidic hydrogen in DPE and TEA, interaction (i) cannot be present and interaction (ii), present in both terminal and non-terminal, is superimposed on interaction (iii).

Acknowledgements

This work was supported by the CONACYT (grant E-3904). S.F-G. thanks Fundacion UNAM and the CONACYT for financial support. A.C. thanks Intercambio Academico UNAM and Universidad Complutense for financial support. We thank Vladimir Dohnal and Jose Manuel Mendez Stivalet for useful discussions.

References

1 M. Costas and D. Patterson, *J. Chem. Soc., Faraday Trans. 1*, 1985, **81**, 635.
2 L. Andreoli-Ball, D. Patterson, M. Costas and M. Caceres-Alonso, *J. Chem. Soc., Faraday Trans. 1*, 1988, **84**, 3991.
3 M. Caceres-Alonso, M. Costas, L. Andreoli-Ball and D. Patterson, *Can. J. Chem.*, 1988, **66**, 989.
4 (*a*) S. Perez-Casas, L. M. Trejo and M. Costas, *J. Chem. Soc., Faraday Trans.*, 1991, **87**, 1733; (*b*) L. M. Trejo, S. Perez-Casas and M. Costas, *J. Chem. Soc., Faraday Trans.*, 1991, **87**, 1739; (*c*) S. Perez-Casas, R. Moreno-Esparza, M. Costas and D. Patterson, *J. Chem. Soc., Faraday Trans.*, 1991, **87**, 1745.
5 D. Salcedo and M. Costas, *J. Chem. Soc., Faraday Trans.*, 1997, **93**, 3781.
6 M. Costas and D. Patterson, *J. Chem. Soc., Faraday Trans. 1*, 1985, **81**, 655.
7 D. D. Deshpande, D. Patterson, L. Andreoli-Ball, M. Costas and L. M. Trejo, *J. Chem. Soc., Faraday Trans.*, 1991, **87**, 1133.
8 M. Costas, Z. Yao and D. Patterson, *J. Chem. Soc., Faraday Trans. 1*, 1989, **85**, 2211.
9 S. Perez-Casas, R. Castillo and M. Costas, *J. Phys. Chem.*, 1997, **101**, 7043.
10 T. M. Letcher, F. E. Z. Schoonbaert, J. Mercer-Chalmers and A. K. Prasad, *Thermochim. Acta*, 1990, **171**, 147.
11 T. M. Letcher, F. E. Z. Schoonbaert and B. Bean, *Fluid Phase Equilib.*, 1990, **61**, 111.
12 T. M. Letcher, J. Mercer-Chalmers, U. P. Govender and S. Radloff, *Thermochim. Acta*, 1993, **224**, 33.
13 T. M. Letcher, J. Mercer-Chalmers and U. P. Govender, *Fluid Phase Equilib.*, 1993, **91**, 313.
14 T. M. Letcher, J. Mercer-Chalmers, S. Schnabel and A. Heintz, *Fluid Phase Equilib.*, 1995, **112**, 131.
15 (*a*) P. Picker, P. A. Leduc, P. R. Philippe and J. E. Desnoyers, *J. Chem. Thermodyn.*, 1971, **3**, 631; (*b*) J. L. Fortier and G. C. Benson, *J. Chem. Thermodyn.*, 1976, **8**, 411.
16 M. Rogalski and S. Malanowski, *Fluid Phase Equilib.*, 1977, **1**, 137.
17 S. Figueroa-Gerstenmaier, A. Cabañas and M. Costas, in preparation.
18 J. Pouchly, *J. Chem. Soc., Faraday Trans. 1*, 1986, **82**, 1605.
19 M. Costas and D. Patterson, *Thermochim. Acta*, 1987, **120**, 161.
20 This laboratory, in preparation.
21 A. Heintz, *Ber. Bunsen-Ges. Phys. Chem.*, 1985, **89**, 172.
22 M. Bender and A. Heintz, *Fluid Phase Equilib.*, 1993, **89**, 197.
23 W. Mier, G. Oswald, E. Tusel-Langer and R. N. Lichtenthaler, *Ber. Bunsen-Ges. Phys. Chem.*, 1995, **99**, 1123.
24 T. Hofman and C. Casanova, *J. Chem. Soc., Faraday Trans.*, 1996, **92**, 1175.
25 M. H. K. Ghassemi, J-P. E. Grolier and H. V. Kehiaian, *J. Chim. Phys.*, 1976, **73**, 925.
26 W. Woycicki, *J. Chem. Thermodyn.*, 1975, **7**, 1007.
27 S. Suzuki, P. G. Creen, R. E. Bumgarner, S. Dasgupta, W. A. Goddard III and G. A. Blake, *Science*, 1992, **257**, 942.
28 R. West and C. S. Kraihanzel, *J. Am. Chem. Soc.*, 1961, **83**, 765.
29 Z. Yoshida, N. Ishibe and H. Ozoe, *J. Am. Chem. Soc.*, 1972, **94**, 4948.
30 S. Murahashi, B. Ryutani and K. Hatada, *Bull. Chem. Soc. Jpn.*, 1959, **32**, 1001.
31 M-L. Josien, P-V. Houng and T. Lascombe, *C.r. Hebdomad Sé. Acad. Sci.*, 1960, **251**, 1379.
32 J. V. Hatton and R. E. Richards, *Trans. Faraday Soc.*, 1961, **57**, 28.
33 J. C. D. Brand, G. Eglinton and J. F. Morman, *J. Chem. Soc.*, 1960, 2526.
34 J. C. D. Brand, G. Eglinton and J. Tyrell, *J. Chem. Soc.*, 1965, 5914.
35 P. de St Romain, H. T. Van and D. Patterson, *J. Chem. Soc., Faraday Trans. 1*, 1979, **75**, 1700.
36 E. Wilhelm, A. Inglese, J-P. E. Grolier and H. V. Kehiaian, *Monatshefte für Chem.*, 1978, **109**, 235.
37 E. Wilhelm, A. Inglese, J-P. E. Grolier and H. V. Kehiaian, *Monatshefte für Chem.*, 1978, **109**, 435.

Paper 8/09049A